

A Deep Generative Learning Approach for Two-stage Adaptive Robust Optimization

Aron Brenner^{*1,3}, Rahman Khorramfar^{1,2}, Jennifer Sun⁴, and Saurabh Amin^{1,2,3}

¹*Laboratory for Information & Decision Systems, Massachusetts Institute of Technology, Cambridge, MA*

²*MIT Energy Initiative, Massachusetts Institute of Technology, Cambridge, MA*

³*Civil and Environmental Engineering, Massachusetts Institute of Technology, Cambridge, MA*

⁴*Electrical Engineering and Computer Science, Massachusetts Institute of Technology, Cambridge, MA*

Abstract

Two-stage adaptive robust optimization is a powerful approach for planning under uncertainty that aims to balance costs of “here-and-now” first-stage decisions with those of “wait-and-see” recourse decisions made after uncertainty is realized. To embed robustness against uncertainty, modelers typically assume a simple polyhedral or ellipsoidal set over which contingencies may be realized. However, these simple uncertainty sets tend to yield highly conservative decision-making when uncertainties are high-dimensional. In this work, we introduce AGRO, a column-and-constraint generation algorithm that performs adversarial generation for two-stage adaptive robust optimization using a variational autoencoder. AGRO identifies realistic and cost-maximizing contingencies by optimizing over spherical uncertainty sets in a latent space using a projected gradient ascent approach that differentiates the optimal recourse cost with respect to the latent variable. To demonstrate the cost- and time-efficiency of our approach experimentally, we apply AGRO to an adaptive robust capacity expansion problem for a regional power system and show that AGRO is able to reduce costs by up to 7.8% and runtimes by up to 77% in comparison to the conventional column-and-constraint generation algorithm.

*Corresponding author. Email: abrenner@mit.edu

1 Introduction

Growing interest in data-driven stochastic optimization has been facilitated by the increasing availability of more granular data for a wide range of settings where decision-makers hedge against uncertainty and shape operational risks through effective planning. Adaptive robust optimization (ARO) – also referred to as adjustable or two-stage/multi-stage robust optimization [İhsan Yanikoğlu et al., 2019] – is one class of models that has found applications in optimization of industrial processes [Gong and You, 2017], transportation systems [Xie et al., 2020], and energy systems planning [Bertsimas et al., 2012]. In this work, we aim to solve data-driven two-stage ARO problems with high-dimensional uncertainty that take the form

$$\min_{x \in \mathcal{X}} \left\{ c^\top x + \lambda \max_{\xi \in \mathcal{U}} \min_{y \in \mathcal{Y}(\xi, x)} d^\top y \right\}. \quad (1)$$

Here, x represents “here-and-now” first-stage decisions while y represents “wait-and-see” recourse decisions made after the random variable $\xi \in \mathbb{R}^D$ is realized. The set $\mathcal{U} \subset \mathbb{R}^D$ represents the *uncertainty set*, encompassing all possible realizations of ξ that must be accounted for when identifying the optimal first-stage decisions x . In this work, we assume first-stage decisions x belongs to a mixed-integer feasible set \mathcal{X} while recourse decisions y belong to a polyhedral set $\mathcal{Y}(\xi, x) = \{y \mid By \geq b(\xi) - A(\xi)x, y \geq 0\}$, where $b(\xi)$ and $A(\xi)$ are affine functions. Additionally, we adopt a *complete recourse* assumption, i.e., $\mathcal{Y}(\xi, x) \neq \emptyset$ for any $\xi \in \mathcal{U}, x \in \mathcal{X}$.

As an illustrative example, consider the problem of *capacity expansion planning* for a supply chain network. In this case, x denotes discrete long-term decisions (i.e., constructing warehouses), which require an upfront investment $c^\top x$. As the day unfolds and demands ξ are known, production and transportation decisions $y \in \mathcal{Y}(\xi, x)$ can be made to meet demand at a recourse cost of $d^\top y$. To ensure robustness against uncertain demand, first-stage decisions balance investment costs with the λ -weighted worst-case daily production and transportation cost incurred over the uncertainty set \mathcal{U} .

The uncertainty set \mathcal{U} plays a large role in shaping planning outcomes and as such must take into account the available data as well as the planner’s risk preferences. To optimize risk measures such as worst-case costs or value-at-risk more precisely, it is advantageous to construct \mathcal{U} based on the desired risk tolerance and obtain probabilistic guarantees on the recourse cost before optimizing. In the case of nonadaptive robust optimization (RO), various probabilistic guarantees can be obtained for a range of conventional (e.g., ellipsoidal, budget) uncertainty sets depending on in the information one has about the distribution of uncertainty p_ξ [Bertsimas et al., 2021, 2023]. These results, which give guarantees for

certain classes of constraints admitting a closed-form expression, are not easily extended to the case of recourse costs in ARO problems. While an approximate α -probability guarantee can be obtained using an uncertainty set that contains α -fraction of ξ observations, such an approach can yield increasingly conservative solutions to (1) – i.e., solutions that “over-invest” in anticipation of extreme contingencies – in settings with high-dimensional uncertainty as the size of such uncertainty sets scale exponentially with D [Lam and Qian, 2019].

In this work, we propose AGRO, a solution algorithm that embeds a variational autoencoder within a column-and-constraint generation (CCG) scheme to perform adversarial generation of realistic contingencies for adaptive robust optimization. We list our contributions below:

- **Extension of deep data-driven uncertainty sets to ARO.** We extend recent approaches for learning tighter uncertainty sets in RO [Hong et al., 2021, Goerigk and Kurtz, 2023, Chenreddy et al., 2022] to the case of ARO, a richer class of optimization models that allows for recourse decisions to be made after uncertainty is realized.
- **ML-assisted optimization using exact solutions.** Rather than approximate decision-making with a predictive model [Bertsimas and Kim, 2023, Dumouchelle et al., 2024], we train a generative model to approximate the distribution of uncertain parameters. Consequently, AGRO does not require building a large dataset of solved problem instances for training a predictive model and optimizes with respect to exact recourse costs rather than an ML-based approximation.
- **Application to planning with observed energy supply/demand data.** We apply our solution algorithm to the problem of long-term power system planning under hourly supply/demand uncertainties – a data-driven setting with high-dimensional and nonlinearly correlated uncertainty – and show reductions in both costs and runtimes when compared to a conventional CCG algorithm.

The remainder of the text is organized as follows. In Sec. 2, we describe the state of the art for modeling with ARO. First, we describe the CCG solution framework and outline standard approaches for uncertainty set construction, which together provide a basis for discussion of recent developments integrating learning and optimization for RO/ARO. In Sec. 3, we describe our solution algorithm in full, which integrates an uncertainty set representation learned by a variational autoencoder (VAE) within the CCG algorithm. Finally, in Sec. 4, we apply our CCG algorithm to the case of capacity expansion planning for a regional power system and compare against the conventional CCG approach.

2 Preliminaries

2.1 Uncertainty Sets

A fundamental modeling decision in both robust optimization and ARO is the definition of the uncertainty set \mathcal{U} , representing the range of uncertainty realizations for which the first stage decision x must be robust. The most widely adopted uncertainty sets are variations of the box, budget, and ellipsoidal uncertainty sets [Bertsimas et al., 2021], which can be obtained in a data-driven setting as

$$\mathcal{U}^{\text{box}} = \left\{ \xi \in \mathbb{R}^D \mid \hat{\xi}^{\min} \leq \xi_i \leq \hat{\xi}^{\max}, \forall i = 1, \dots, D \right\} \quad (2a)$$

$$\mathcal{U}^{\text{budget}} = \left\{ \xi \in \mathbb{R}^D \mid \sum_{i=1}^D \hat{\Sigma}_{ii}^{-1} |\xi_i - \hat{\mu}_i| \leq \Gamma_{\text{budget}} \right\} \quad (2b)$$

$$\mathcal{U}^{\text{ellipse}} = \left\{ \xi \in \mathbb{R}^D \mid (\xi - \hat{\mu})^\top \hat{\Sigma}^{-1} (\xi - \hat{\mu}) \leq \Gamma_{\text{ellipse}} \right\}. \quad (2c)$$

Here, $\hat{\mu}$, $\hat{\Sigma}$, $\hat{\xi}^{\min}$, and $\hat{\xi}^{\max}$ denote the empirical mean, covariance, minimum value, and maximum value of the empirical distribution of ξ while the Γ parameters denote the uncertainty “budgets.” To obtain an approximate α -probability guarantee of feasibility, one can select Γ such that \mathcal{U} covers an α -fraction of observed ξ realizations. Alternatively, one can take a distributionally robust approach to selecting Γ by leveraging concentration inequalities.

2.2 Column-and-Constraint Generation

Once \mathcal{U} is defined, one can apply a number of methods to either exactly [Zeng and Zhao, 2013, Thiele et al., 2009] or approximately [Kuhn et al., 2011] solve the ARO problem. Here, we focus our discussion on the CCG algorithm [Zeng and Zhao, 2013] due to its prevalence in the ARO literature (including its use in recent learning-assisted methods [Bertsimas and Kim, 2023, Dumouchelle et al., 2024]) and because it provides a nice foundation for introducing AGRO in Sec. 3. The CCG algorithm is an exact solution method for ARO that iteratively identifies “worst-case” uncertainty realizations ξ^i by maximizing recourse costs for a given first-stage decision x^* . These uncertainty realizations are added in each iteration to the finite

scenario set \mathcal{S} , which is used to instantiate the *main problem*

$$\begin{aligned}
\min_{x, y, \gamma} \quad & c^\top x + \lambda \gamma \\
\text{s.t.} \quad & x \in \mathcal{X} \\
& A(\xi^i)x + By^i \geq b(\xi^i) && \xi^i \in \mathcal{S} \\
& y^i \geq 0 && i = 1, \dots, |\mathcal{S}| \\
& \gamma \geq d^\top y^i && i = 1, \dots, |\mathcal{S}|
\end{aligned}$$

where γ denotes the worst-case recourse cost over \mathcal{S} (see (1)). In each iteration i of the CCG algorithm, additional variables (i.e., columns) y^i and constraints $y^i \in \mathcal{Y}(\xi^i, x)$ corresponding to the most recently identified worst-case realization are added to the main problem.

Solving the main problem yields a set of first-stage decisions, x^* , which are fixed as parameters in the *adversarial subproblem*

$$\max_{\xi \in \mathcal{U}} \min_{y \geq 0} \{d^\top y \mid By \geq b(\xi) - A(\xi)x^*\}. \tag{3}$$

Solving the adversarial subproblem yields a new worst-case realization ξ^i to be added to \mathcal{S} . Such a max-min problem can be solved by constructing the dual of the inner minimization problem and maximizing $d^\top y$ subject to Karush–Kuhn–Tucker (KKT) conditions of the inner minimization problem [Zeng and Zhao, 2013]. Despite its prominence in the literature, the KKT reformulation of (3) yields a potentially large bilinear problem; specifically, one for which the number of bilinear terms scales linearly with D . This need to repeatedly solve a large-scale bilinear program can cause CCG to be computationally unwieldy in the case of high-dimensional uncertainty. To this end, a number of alternative solution approaches – including some that leverage ML methods – have been proposed that approximate recourse decisions in order to yield more tractable reformulations, which we discuss next.

2.3 Learning for Adaptive and Single-stage RO

As an alternative to CCG and other exact methods, linear decision rules (LDRs) are commonly used to approximate recourse decisions as affine functions of uncertainty [Kuhn et al., 2011]. To better approximate recourse costs using a richer class of functions, Rahal et al. [2022] propose a “deep lifting” procedure with neural networks to learn piecewise LDRs. Bertsimas and Kim [2023] train decision trees to predict near-optimal first-stage decisions, worst-case uncertainty, and recourse decisions, which are deployed as part of a solution algorithm for ARO. Similarly, Dumouchelle et al. [2024] train a neural network to approximate optimal

recourse costs conditioned on first-stage decisions, which they embed within a CCG-like algorithm.

While these learning-assisted methods address some shortcomings of conventional methods (such as CCG) in reducing runtimes, several challenges remain. The first of these is *looseness* of uncertainty representation. These methods, along with the conventional CCG algorithm, fail to address the challenge of “loose” uncertainty sets which arises in the case of high-dimensional uncertainty. While uncertainty sets of the form (2) may be effective in approximating high-density regions in low-dimensional settings, they are prone to yielding costly, overly conservative solutions when ξ is high-dimensional [Lam and Qian, 2019]. The second such challenge is *inexactness*; specifically, these methods optimize first-stage decisions with regard to a learned approximation of the recourse cost rather than the actual recourse cost, $\min_{y \in \mathcal{Y}(\xi, x)} d^\top y$. Accordingly, the quality of the approximation depends on the extensiveness of pre-training and amount of training data matching (ξ, x) pairs to corresponding recourse costs. Obtaining such training data in particular can be computationally onerous as it involves solving a large number of linear programs.

In the case of nonadaptive RO, some recent works have addressed the issue of looseness by learning “deep data-driven” uncertainty sets. Hong et al. [2021] propose using clustering and dimensionality reduction methods to construct data-driven uncertainty sets as unions or intersections of ellipsoids and polyhedra. More similarly to our work, Goerigk and Kurtz [2023] introduce a solution algorithm that first constructs a tight uncertainty set as the image of a Gaussian superlevel set under a neural network-learned transformation and then iteratively identifies worst-case realizations by optimizing “through” the neural network. Chenreddy et al. [2022] extend their approach to construct uncertainty sets conditioned on the observation of a subset of covariates. In these two studies, the adversarial subproblem corresponds to a tractable mixed-binary linear program with as many binary variables as hidden units in the neural network. While Goerigk and Kurtz [2023] and Chenreddy et al. [2022] show their deep data-driven uncertainty set approach reduces costs in the case of nonadaptive RO, these approaches cannot be easily extended to ARO. This is because the resulting subproblem will correspond to a max-min problem, which does not admit a tractable duality-based reformulation due to the presence of binary variables.

3 AGRO

In this work, we propose AGRO, a solution algorithm that performs adversarial generation for robust optimization. As described in Fig. 1, AGRO modifies the conventional CCG algorithm in two key ways: (1) To reduce looseness (and by consequence, costs) we construct

an uncertainty set with (approximately) known probability mass by training a VAE and projecting spherical uncertainty sets from the latent space into the space of ξ . (2) Because the recourse cost does not admit a closed-form expression, the adversarial subproblem cannot be formulated as a mixed-integer program as was the case in [Goerigk and Kurtz, 2023, Chenreddy et al., 2022]. Consequently, we solve the subproblem by differentiating the recourse cost with respect to ξ and performing gradient ascent to identify worst-case realizations.

Table 1: Related works on RO and ARO.

Studies	Problem	Exact Recourse	ML-Based Uncertainty	Subproblem	Training Data
[Zeng and Zhao, 2013] [Thiele et al., 2009]	ARO	✓		Bilevel Program	—
[Goerigk and Kurtz, 2023] [Chenreddy et al., 2022]	RO	—	✓	Mixed-binary Linear Program	Realizations
[Dumouchelle et al., 2024]	ARO			Mixed-binary Linear Program	Solutions
AGRO	ARO	✓	✓	Nonconcave Maximization	Realizations

Table 1 compares AGRO to related works for ARO and single-stage RO. Our approach is similar to that of [Dumouchelle et al., 2024] in that we optimize “through” a trained neural network to obtain worst-case scenarios within a CCG algorithm. While [Dumouchelle et al., 2024] approximate recourse decisions using a predictive model to reduce runtime, however, we *exactly* solve the recourse problem as a linear program in each iteration while leveraging a trained VAE to approximate the distribution of uncertainty. Doing so also removes the computational effort required for building a dataset of recourse problem solutions – i.e., solving a large number of linear programs to obtain an accurate predictive model for recourse cost given ξ and x . Additionally, our approach extends the work of [Goerigk and Kurtz, 2023] and [Chenreddy et al., 2022] in constructing tighter uncertainty sets using deep learning to the problem setting of ARO.

3.1 Deep Data-Driven Uncertainty Sets

Toward addressing the challenge of looseness, we take a VAE approach to learning tight uncertainty sets as nonlinear and differentiable transformations of convex uncertainty sets lying in the latent space \mathbb{R}^L with $L < D$. We let $z \sim p_z = \mathcal{N}(0, I_L)$ be an isotropic Gaussian random variable and let $h_\phi : \mathbb{R}^L \rightarrow \mathbb{R}^D$ and $g_\theta : \mathbb{R}^L \rightarrow \mathbb{R}^D$ respectively denote the encoder and decoder of a variational autoencoder (VAE) model trained to generate

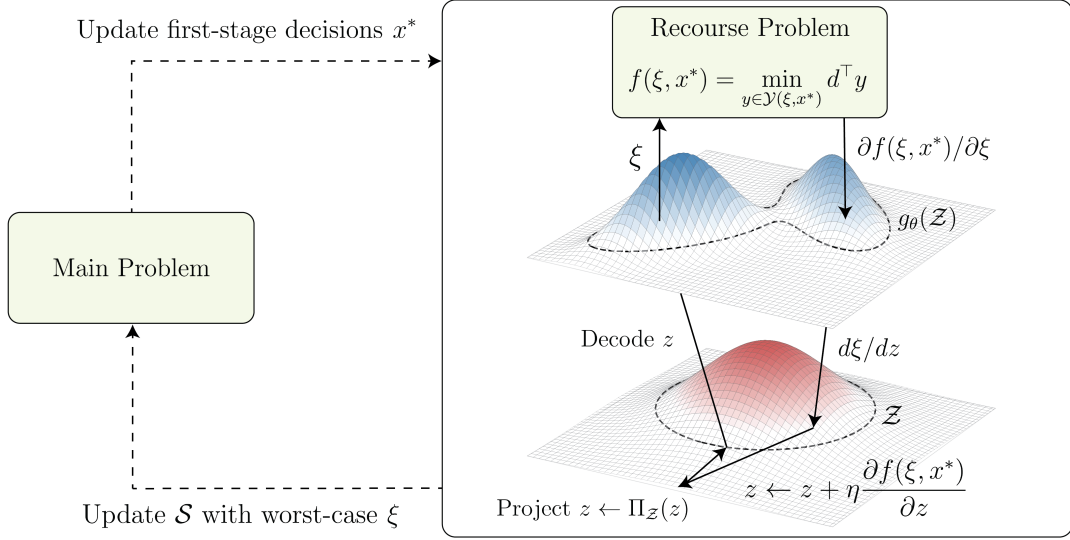


Figure 1: The proposed AGRO solution algorithm. (i) First-stage decisions x^* are obtained by solving a main problem for a finite set of uncertainty realizations, \mathcal{S} . (ii) z is sampled from within \mathcal{Z} and decoded to obtain an initial ξ . (iii) The recourse problem is solved given x^* and ξ and its optimal objective value is differentiated with respect to ξ , and by applying the chain rule, z . (iv) A gradient ascent step is taken to update z , which is then projected onto \mathcal{Z} and decoded to obtain an updated ξ . Steps (iii) and (iv) are iterated until converging to a worst-case ξ . (v) The worst-case ξ is then added to \mathcal{S} , at which point the main problem is re-optimized.

samples from p_ξ [Kingma and Welling, 2013]. Specifically, h_ϕ is trained to map samples of uncertainty realizations to samples from the isotropic Gaussian distribution while g_θ is trained to perform the reverse mapping. Here, L denotes the VAE bottleneck dimension, which is a hyperparameter that significantly influences the diversity and quality of generated samples and is generally tuned through a process of trial and error. We note that our approach can be extended to other classes of deep generative models that learn such a mapping from $\mathcal{N}(0, I_L)$ to p_ξ such as generative adversarial networks [Goodfellow et al., 2014], normalizing flows [Papamakarios et al., 2021], and diffusion models [Ho et al., 2020]. However, we employ a VAE architecture as such models are known to exhibit relatively high stability in training and low computational effort for sampling [Bond-Taylor et al., 2021], making them highly conducive to integration within an optimization framework.

We let \mathcal{Z} be the L -ball $\mathcal{B}(0, r)$ with r chosen to be the minimum value such that an α -fraction of projected uncertainty realizations $h_\phi(\xi)$ are observed to fall within \mathcal{Z} . Since \mathcal{Z} is closed and bounded, the image of \mathcal{Z} under g_θ , which is continuous, will also be a closed and bounded (but not necessarily convex) set $g_\theta(\mathcal{Z}) \in \mathbb{R}^D$. Unless g_θ is also invertible, the probability mass contained in this set under p_ξ will not necessarily equal α , the sample estimate of probability mass in \mathcal{Z} under p_z [Papamakarios et al., 2021]. Nevertheless, we

observe that constraining z to \mathcal{Z} (and by extension, ξ to $g_\theta(\mathcal{Z})$) discourages generating uncertainty realizations that are unrealistic or lie outside of high-density regions of p_ξ . This is intuitive as realizations lying farther from the origin in the latent space are estimated to have lower likelihood under the VAE Gaussian prior [Kingma and Welling, 2013]. Fig. 2 shows a comparison of conventional uncertainty sets against a tighter uncertainty set constructed by the proposed VAE-based method for samples from the bivariate “moons” distribution [Pedregosa et al., 2011].

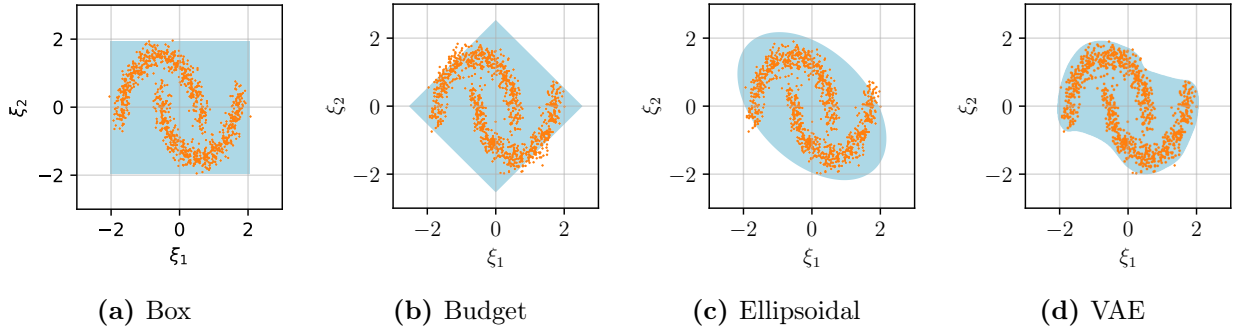


Figure 2: Uncertainty sets (blue) constructed to cover at least 95% of realizations (orange).

3.2 Adversarial Subproblem

Given a decoder (i.e., generative model) $g_\theta : \mathbb{R}^L \rightarrow \mathbb{R}^D$, latent uncertainty set $\mathcal{Z} = \mathcal{B}(0, r)$, and first-stage decision x^* , we then formulate the adversarial subproblem as

$$\max_{z \in \mathcal{Z}} \min_y \{d^\top y \mid By^i \geq b(g_\theta(z)) - A(g_\theta(z))x^*\}, \quad (4)$$

which substitutes $g_\theta(z)$ and \mathcal{Z} for ξ and \mathcal{U} respectively in (3). We denote the optimal objective value of the recourse problem as a function of ξ by $f : \mathbb{R}^D \rightarrow \mathbb{R}$ (see Fig. 1). It is then possible to differentiate f with respect to ξ by implicitly differentiating the optimality conditions of the recourse problem at an optimal solution [Amos and Kolter, 2017]. Doing so provides an ascent direction for maximizing f with respect to ξ , and by applying the chain rule, z , which can be leveraged to maximize f using first-order optimization methods. By maximizing f using projected gradient ascent over \mathcal{Z} , we discourage selection of worst-case realizations that fall outside high-density regions of p_ξ .

Importantly, projected gradient ascent is not guaranteed to converge to a worst-case uncertainty realization as solving $\max_z f(g_\theta(z), x^*)$ requires maximizing the composition of f , which is convex [Boyd and Vandenberghe, 2004], with g_θ , which is not necessarily convex nor concave. As such, the adversarial problem requires maximizing a nonconcave function, which

does not yield convergence guarantees to global maxima. To encourage discovery of global maxima, we solve the adversarial subproblem multiple times in each iteration with I different, random initializations of z . Specifically, each initialization requires that we first randomly sample a latent variable z from a distribution p_s (e.g., the truncated normal or uniform distribution) supported on \mathcal{Z} . We then transform z to obtain the uncertainty realization $\xi = g_\theta(z)$ and solve the inner linear minimization problem with respect to ξ to obtain $f(\xi, x^*)$ and $\partial f/\partial \xi$. Using automatic differentiation, we obtain the gradient of ξ with respect to z and perform the update

$$z \leftarrow \Pi_{\mathcal{Z}} \left(z + \eta \frac{\partial f(\xi, x^*)}{\partial \xi} \frac{d\xi}{dz} \right),$$

where $\eta > 0$ denotes the step-size hyperparameter and $\Pi_{\mathcal{Z}}$ denotes the projection operator given by

$$\Pi_{\mathcal{Z}}(z) = \begin{cases} z, & z \in \mathcal{Z} \\ r \cdot \frac{z}{\|z\|_2}, & z \notin \mathcal{Z}. \end{cases}$$

This procedure is repeated until a convergence criterion is met. At this point, the worst-case uncertainty realization obtained over all I initializations is added to \mathcal{S} and the main problem is re-optimized, which completes one iteration of the AGRO solution algorithm. AGRO terminates when the worst-case total costs estimated by the main problem and subproblem have converged, i.e., $\frac{(c^\top x^* + \lambda f(\xi^i, x^*)) - (c^\top x^* + \lambda \gamma)}{c^\top x^* + \lambda \gamma} \leq \epsilon$ for some convergence tolerance ϵ . The full pseudocode for AGRO is now presented in Alg. 2.

4 Application to Capacity Expansion Planning

Stochastic capacity expansion models have become a centerpiece for long-term planning of energy generation, transmission, and distribution infrastructure under supply, demand, and cost uncertainties [Zhang et al., 2024, Roald et al., 2023]. A number of recent works have adopted ARO formulations for future energy systems planning with a particular focus on ensuring system reliability under mass adoption of renewable energy with intermittent and uncertain supply [Ruiz and Conejo, 2015, Amjady et al., 2017, Minguez et al., 2017, Abdin et al., 2022]. In capacity expansion settings with high spatiotemporal fidelities, supply and demand uncertainties are complex, high-dimensional, and nonunimodal, exhibiting nonlinear correlations such as temporal autocorrelations and spatial dependencies. These patterns cannot be accurately captured by conventional uncertainty sets such as those introduced

Algorithm 2 AGRO Algorithm

Require: Decoder g_θ , Confidence Level α , Step-size η , Initializations I , Convergence tolerance ϵ

Ensure: Optimal solution x^*

```
1: Initialize Scenario set  $\mathcal{S} \leftarrow \emptyset$ , Iteration counter  $i \leftarrow 1$ 
2: while not converged do
3:    $x^*, \gamma \leftarrow \operatorname{argmin}_{x \in \mathcal{X}, \gamma} \{f(x) + \gamma \mid f(\xi^i, x) \leq \gamma, \forall \xi^i \in \mathcal{S}\}$  ▷ Solve main problem
4:   for  $j = 1$  to  $I$  do ▷ Solve adversarial subproblem
5:     Sample  $z^j \sim p_s$ 
6:     while not converged do
7:       Decode  $\xi = g_\theta(z^j)$ 
8:       Solve recourse problem for  $f(\xi, x^*)$ 
9:        $z^j \leftarrow \Pi_{\mathcal{Z}} \left( z^j + \eta \frac{\partial f(\xi, x^*)}{\partial \xi} \frac{d\xi}{dz^j} \right)$ 
10:    end while
11:  end for
12:   $j^* \leftarrow \operatorname{argmax}_{j \in \{1, \dots, I\}} f(g_\theta(z^j), x^*)$  ▷ Select worst-case realization
13:  Set  $\xi^i \leftarrow g_\theta(z^{j^*})$ 
14:  if  $f(\xi^i, x^*) \leq \gamma$  then ▷ Check convergence
15:    Terminate and return  $x^*$ 
16:  else
17:    Update  $\mathcal{S} \leftarrow \mathcal{S} \cup \{\xi^i\}$  ▷ Add worst-case realization to scenario set
18:    Increment  $i \leftarrow i + 1$ 
19:  end if
20: end while
21: return  $x^*$ 
```

in (2). As a result, tightening uncertainty representations for robust capacity expansion planning has the potential to significantly lower investment costs over conventional ARO methods while still maintaining low operational costs day-to-day.

In this section, we apply AGRO to a two-stage adaptive robust generation and transmission expansion planning problem for the New England transmission system. We assume a data-driven setting with high-dimensional uncertainty corresponding to hourly demand as well as solar, onshore wind, and offshore wind capacity factors (average power output divided by the plant’s maximum production capacity) at each node. Our results demonstrate AGRO’s ability to reduce both costs and runtimes when compared to solutions obtained by the CCG algorithm. In what follows, we briefly describe the adaptive robust generation and transmission expansion problem and leave the complete formulation in Appendix. A.

4.1 Formulation

The generation and transmission expansion problem we present most closely follows that of [Minguez et al., 2017] and has two stages: an initial investment stage and a subsequent economic dispatch (i.e., recourse) stage. The objective function is a weighted sum of investment

costs plus annualized worst-case economic dispatch costs. Investment decisions are made at the node level and include installed capacities for (1) dispatchable, solar, onshore wind, and offshore wind power plants at each node; (2) battery storage at each node; (3) transmission lines. In the first stage, the capacity of new dispatchable and renewable power plants as well as new transmission lines are constrained by their respective upper bounds. The economic dispatch stage occurs after the realization of uncertain demand and supply. This stage determines optimal hourly generation, power flow, and storage decisions to minimize the combined cost of load shedding and variable cost for dispatchable generation; these decisions are subject to ramping, storage, and flow balance constraints. To simulate inter-day dynamics of storage and ramping, we implement circular indexing, which links battery state-of-charge and dispatchable generation rates at the end of the day with those at the beginning [Jacobson et al., 2024].

4.2 Experimental Setup

In our experiments, we utilize hourly demand and capacity factor projections for a six-node zonal representation of New England, which yields an uncertain random variable ξ with 349 distinct features after data processing (see B.1) [Khorramfar et al., 2024]. We segment the dataset to perform a five-fold cross-validation with each fold having a held-out set of 1000 samples and report cross-validated estimates of total costs. Specifically, for a given fold, we train one VAE using an 80/20 training/validation split on the in-sample data, solve the ARO problem using Alg. 2, and obtain an out-of-sample cost estimate in each iteration by fixing x^* and computing $c^\top x^* + \lambda \hat{F}^{-1}(\alpha)$, where $\hat{F}^{-1}(\alpha)$ is the out-of-sample α -quantile estimate of $f(\xi, x^*)$.

As a baseline method, we report results for CCG using an uncertainty set constructed from the intersection of the budget and box uncertainty sets (see (2)), which is commonly used in the power systems literature [Bertsimas et al., 2012, Ruiz and Conejo, 2015, Amjady et al., 2017, Abdin et al., 2022]. For our experiments, Γ is selected such that \mathcal{U} covers $\alpha = 95\%$ of the training set. For AGRO, we likewise select r such that the uncertainty set $\mathcal{Z} = \mathcal{B}(0, r)$ covers 95% of the training set after being projected by h_ϕ into the L -dimensional latent space. Additionally, we report results for a range of latent dimensionalities, $L \in \{2, 4, 8, 16\}$. Additional details regarding the VAE architecture and training setup are given in Appendix B.2

Method	Objective			Runtime			
	Sample Est.	Main Prob.	Error	Total	Training	SP	Iter.
CCG	1.03×10^{10}	1.31×10^{10}	78.6%	1487	—	14	23
AGRO ($L = 2$)	9.50×10^9	9.82×10^9	18.8%	341	184	18	5
AGRO ($L = 4$)	9.58×10^9	1.14×10^{10}	35.9%	894	185	90	7
AGRO ($L = 8$)	9.86×10^9	1.23×10^{10}	35.3%	1110	187	133	6
AGRO ($L = 16$)	9.71×10^9	1.36×10^{10}	49.3%	1837	193	206	7

Table 2: Capacity expansion cost estimates and runtimes (in seconds) averaged over all folds. “Sample Est.” denotes the sample-estimated objective value, $c^\top x^* + \lambda \hat{F}^{-1}(\alpha)$, while “Main Prob.” denotes the objective value obtained in the final iteration, $c^\top x^* + \lambda \gamma$. “Error” denotes the mean absolute percent error of approximated worst-case recourse costs obtained by the subproblem (compared to sample-estimated costs) averaged over all iterations. “SP” denotes the runtime for the subproblem averaged over all iterations.

4.3 Results

Cost and runtime. Results for AGRO and CCG costs and runtimes are shown in Table 2. Regarding planning costs, we observe that AGRO obtains investment decisions that yield lower costs than CCG as evaluated by out-of-sample estimates. In particular, costs are minimized by AGRO with $L = 2$ (yielding a 7.8% reduction in costs over CCG) and appear to increase with L . AGRO with $L = 2$ also obtains the lowest total runtime, which includes both VAE training and optimization, while CCG obtains the highest total runtime (approximately 4.4 times that of AGRO with $L = 2$). We also find that the CCG subproblem is solved more quickly than the AGRO subproblem, whose runtime we observe to increase with L . We note that the AGRO subproblem includes multiple initializations of z , which causes its runtime to vary as more initializations are required in later iterations to obtain a new worst-case realization.

Approximation of value-at-risk. Besides sample-estimated costs, we also compare the accuracy of all methods in approximating value-at-risk (VaR), a risk measure that quantifies near worst-case costs, defined by $\min\{\beta \in \mathbb{R} \mid \mathbb{P}_\xi(f(\xi, x) \leq \beta) > \alpha\}$. First, we compare the final objective value, $c^\top x^* + \lambda \gamma$ with x^* and γ obtained from the final iteration of solving, against the sample-estimated cost. We observe that, for all methods, the final objective value is greater than the out-of-sample recourse cost estimate. We also report the mean absolute percent error of the main problem objective value, i.e., $c^\top x^* + \lambda \gamma$, compared to the out-of-sample estimate across all iterations. For both quantities, we observe that AGRO is able to obtain a much tighter estimate of VaR than CCG, which yields an average error of 78.6% over the course of solving. The looseness of this approximation explains the high costs obtained by CCG. Specifically, the identification of improbable but cost-maximizing

uncertainty realizations results in consistent over-estimation of VaR and subsequent over-investment as CCG aims to reduce costs for these improbable realizations. We dedicate the remainder of this subsection to more precisely understanding how AGRO improves over CCG in tightly approximating VaR and consequently reducing costs.

We first visualize the relative performance in approximating VaR for all methods in Fig. 3, which plots the estimated worst-case cost obtained from solving the subproblem $f(\xi^i, x^*)$ against the out-of-sample estimate $\hat{F}^{-1}(\alpha)$ for all iterations of solving in all five folds of cross-validation. We also show standard metrics of generative model fidelity (i.e., precision, density) and diversity (i.e., recall, coverage) for the VAE models in Table 3. Additional details regarding these metrics based on [Naeem et al., 2020] are provided in Appendix B.3. From Fig. 3, we first observe that $f(\xi^i, x^*)$ and $\hat{F}^{-1}(\alpha)$ are highly correlated, which suggests that maximizing the recourse cost serves as a useful proxy for estimating VaR. We also observe that in all cases except AGRO with $L = 2$, $f(\xi^i, x^*)$ is almost always greater than $\hat{F}^{-1}(\alpha)$. This is intuitive as the uncertainty set is designed to contain an α -fraction of realizations, and consequently, the worst-case recourse cost obtained over this set will provide a “safe” approximation (i.e., over-estimate) of VaR at level α . This over-estimating effect is also reflected in the consistent gap between the final objective value and the out-of-sample cost estimate (see Table 2). This is not the case, however, with $L = 2$ as the associated VAE models obtain a much lower coverage than those for $L > 2$ (see Table 3). As such, the uncertainty set does not sufficiently cover the high-density region of p_ξ , which leads to occasional under-estimation of VaR. AGRO with $L = 2$ nevertheless obtains the lowest sample-estimated costs of all methods. Together, these results suggests that, while poor VAE fidelity or diversity can cause AGRO to fail to identify cost-maximizing realizations, the end result is not necessarily a consistent under-estimation of VaR. This is a consequence of the “safe” uncertainty set, which introduces a systemic over-estimating effect with regard to VaR and counteracts the systemic under-estimation resulting from diminished VAE diversity and fidelity. These results highlight the dependence of solution quality on VAE performance while also demonstrating that the ideal choice of L is not necessarily one that maximizes sample fidelity and diversity, and consequently, should be tuned with consideration of downstream optimization outcomes.

L	Precision	Recall	Density	Coverage
2	0.84	0.09	1.06	0.49
4	0.88	0.19	1.39	0.72
8	0.95	0.32	1.73	0.85
16	0.94	0.38	1.58	0.87

Table 3: Averaged VAE performance metrics [Naeem et al., 2020].

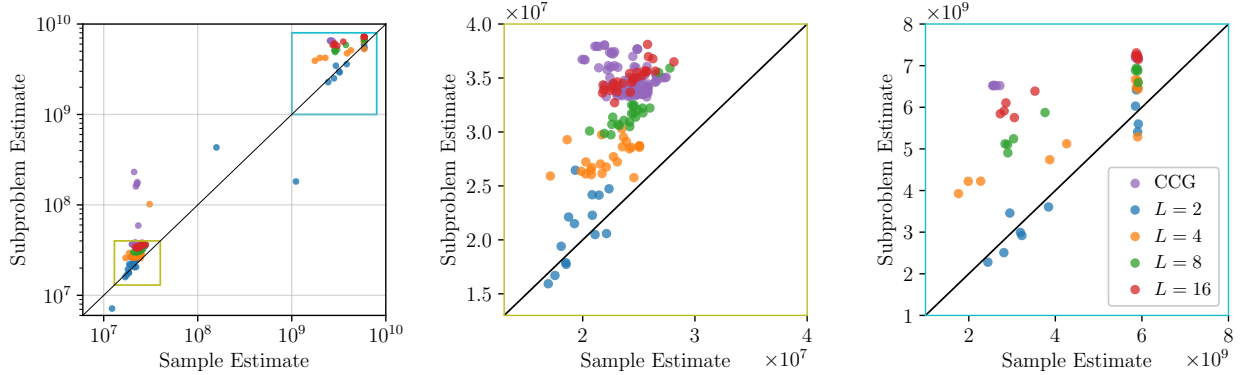
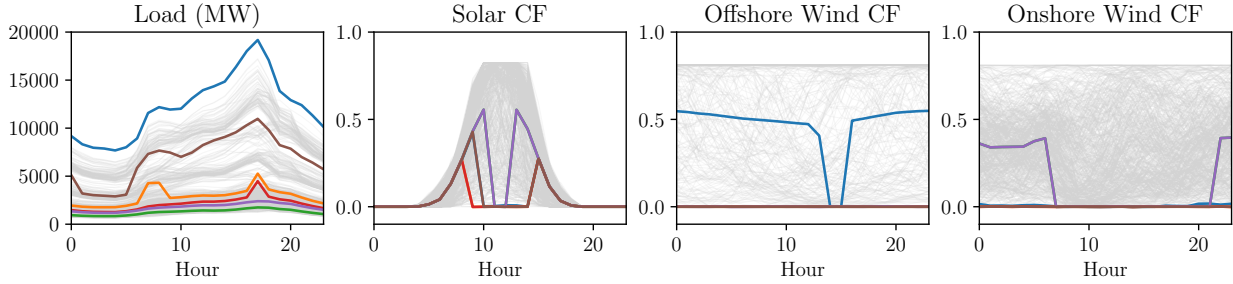


Figure 3: Comparison of sample-estimated VaR, $\hat{F}^{-1}(\alpha)$, and estimated worst-case costs obtained from solving the adversarial subproblem, $f(\xi^i, x^*)$. Each point is obtained from one iteration of AGRO/CCG. Points that are closer to the diagonal line indicate a more accurate estimate of VaR. The middle and right-hand plots provide a zoomed-in view of two regions with a high concentration of points. Subproblem estimates are almost always greater than sample estimates except in the case of AGRO with $L = 2$ (blue).

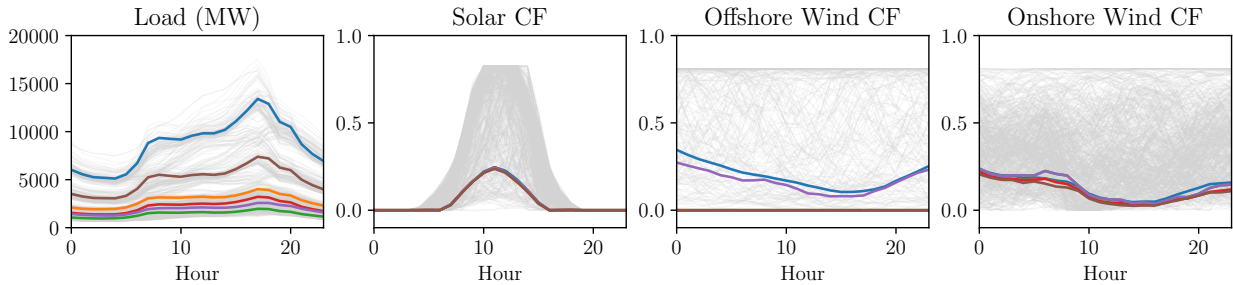
Visualizing worst-case uncertainty. Towards understanding how different uncertainty sets impact conservatism of first-stage decision-making, we compare samples of obtained worst-case realizations in Fig. 4. Specifically, we plot the solution to the adversarial subproblem for the final iteration of one fold of cross-validation for CCG and AGRO with $L = 2$ and $L = 16$. Fig. 4a demonstrates the way in which worst-case realizations obtained by CCG using a budget uncertainty set are unrealistically adversarial. In particular, CCG generates an uncertainty realization in which solar and wind capacity factors drop sharply to zero before immediately rising to their nominal values. Additionally, weather-related correlations between variables are not maintained; most notably, the positive correlation between load and solar capacity factors as well as the spatial correlation of load across the system are not observed. Accounting for these supply and demand features during investment planning is essential for effectively leveraging the complementarities between generation, storage, and transmission. On the other hand, AGRO is able to identify uncertainty realizations that are simultaneously cost-maximizing and realistic. This can be observed from the way in which selected realizations demonstrate realistic temporal autocorrelation (i.e., smoothness) and show a less improbable combination of low solar capacity factors with moderate load.

Comparing the two AGRO-generated realizations, we observe that the $L = 16$ case yields a more cost-maximizing realization than the $L = 2$ case. In particular, loads are higher while capacity factors are lower. Additionally, the generated load and capacity factor time series in the $L = 2$ case are smoother than those in the $L = 16$ case, which can result in under-estimation of load shedding costs resulting from highly fluctuating loads and under-investment in dispatchable generation. These observations, which reflect the fidelity and

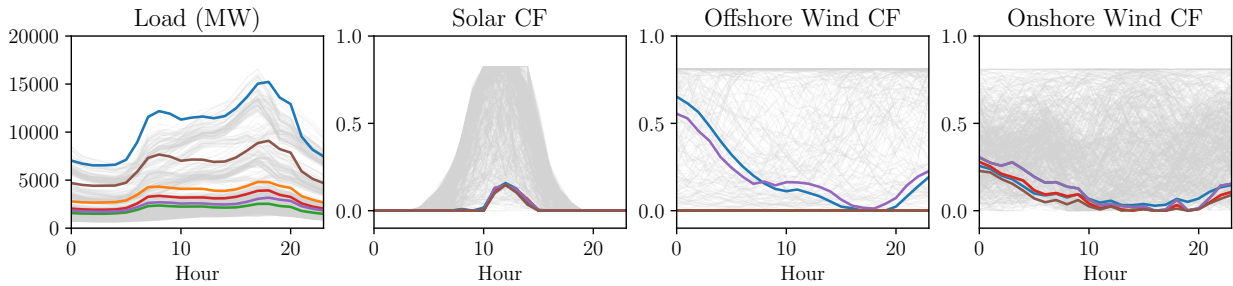
density results shown in Table 3, explain the occasional under-estimation of recourse costs by AGRO with $L = 2$ (see Fig. 3) as well as the lower overall costs resulting from reduced conservatism (see Tab. 2).



(a) CCG Uncertainty Realization



(b) AGRO ($L = 2$) Uncertainty Realization



(c) AGRO ($L = 16$) Uncertainty Realization

Figure 4: Comparison of worst-case uncertainty realizations as obtained by (a) CCG, (b) AGRO ($L = 2$), and (c) AGRO ($L = 16$). Different colors are used to represent each of the six nodes in the power system. Realizations corresponding to a random sample of 100 observations are shown in gray.

5 Conclusion

Increasing availability of data for operations of large-scale systems has inspired growing interest in data-driven optimization. In this work, we extend learning-based approaches for more precise uncertainty representation to the setting of ARO, a powerful framework for planning under uncertainty. We propose AGRO, a modification of the conventional

column-and-constraint generation algorithm for chance-constrained ARO problems. AGRO takes a gradient ascent approach to maximizing the value of the inner minimization problem using differentiable convex optimization and adds worst-case uncertainty realizations to a master problem. By leveraging a VAE to project spherical uncertainty sets from a latent space to nonconvex uncertainty sets in a higher dimensional uncertainty space, AGRO identifies worst-case realizations that are not only adversarial but also more likely to occur than those identified from conventional uncertainty sets. Finally, we applied AGRO to the case of capacity expansion planning under supply/demand uncertainty to experimentally demonstrate AGRO’s efficacy in greatly reducing both costs and runtimes for ARO.

References

- Adam F Abdin, Aakil Caunhye, Enrico Zio, and Michel-Alexandre Cardin. Optimizing generation expansion planning with operational uncertainty: A multistage adaptive robust approach. *Applied Energy*, 306:118032, 2022.
- Akshay Agrawal, Brandon Amos, Shane Barratt, Stephen Boyd, Steven Diamond, and Zico Kolter. Differentiable convex optimization layers, 2019.
- Nima Amjady, Ahmad Attarha, Shahab Dehghan, and Antonio J Conejo. Adaptive robust expansion planning for a distribution network with DERs. *IEEE Transactions on Power Systems*, 33(2):1698–1715, 2017.
- Brandon Amos and J Zico Kolter. Optnet: Differentiable optimization as a layer in neural networks. In *International Conference on Machine Learning*, pages 136–145. PMLR, 2017.
- Dimitris Bertsimas and Cheol Woo Kim. A machine learning approach to two-stage adaptive robust optimization, 2023.
- Dimitris Bertsimas, Eugene Litvinov, Xu Andy Sun, Jinye Zhao, and Tongxin Zheng. Adaptive robust optimization for the security constrained unit commitment problem. *IEEE transactions on power systems*, 28(1):52–63, 2012.
- Dimitris Bertsimas, Dick den Hertog, and Jean Pauphilet. Probabilistic guarantees in robust optimization. *SIAM Journal on Optimization*, 31(4):2893–2920, 2021. doi: 10.1137/21M1390967.
- Dimitris Bertsimas, Dick den Hertog, Jean Pauphilet, and Jianzhe Zhen. Robust convex optimization: A new perspective that unifies and extends. *Mathematical Programming*, 200(2):877–918, 2023.

- Sam Bond-Taylor, Adam Leach, Yang Long, and Chris G Willcocks. Deep generative modelling: A comparative review of vaes, gans, normalizing flows, energy-based and autoregressive models. *IEEE transactions on pattern analysis and machine intelligence*, 44 (11):7327–7347, 2021.
- Stephen P Boyd and Lieven Vandenberghe. *Convex optimization*. Cambridge university press, 2004.
- Abhilash Reddy Chenreddy, Nymisha Bandi, and Erick Delage. Data-driven conditional robust optimization. In S. Koyejo, S. Mohamed, A. Agarwal, D. Belgrave, K. Cho, and A. Oh, editors, *Advances in Neural Information Processing Systems*, volume 35, pages 9525–9537. Curran Associates, Inc., 2022.
- Justin Dumouchelle, Esther Julien, Jannis Kurtz, and Elias B. Khalil. Neur2ro: Neural two-stage robust optimization, 2024.
- Marc Goerigk and Jannis Kurtz. Data-driven robust optimization using deep neural networks. *Computers & Operations Research*, 151:106087, 2023.
- Jian Gong and Fengqi You. Optimal processing network design under uncertainty for producing fuels and value-added bioproducts from microalgae: two-stage adaptive robust mixed integer fractional programming model and computationally efficient solution algorithm. *AIChE Journal*, 63(2):582–600, 2017.
- Ian J. Goodfellow, Jean Pouget-Abadie, Mehdi Mirza, Bing Xu, David Warde-Farley, Sherjil Ozair, Aaron Courville, and Yoshua Bengio. Generative adversarial networks, 2014.
- Gurobi Optimization, LLC. Gurobi Optimizer Reference Manual, 2023.
- Jonathan Ho, Ajay Jain, and Pieter Abbeel. Denoising diffusion probabilistic models. In H. Larochelle, M. Ranzato, R. Hadsell, M.F. Balcan, and H. Lin, editors, *Advances in Neural Information Processing Systems*, volume 33, pages 6840–6851. Curran Associates, Inc., 2020.
- L Jeff Hong, Zhiyuan Huang, and Henry Lam. Learning-based robust optimization: Procedures and statistical guarantees. *Management Science*, 67(6):3447–3467, 2021.
- Anna Jacobson, Filippo Pecci, Nestor Sepulveda, Qingyu Xu, and Jesse Jenkins. A Computationally Efficient Benders Decomposition for Energy Systems Planning Problems with Detailed Operations and Time-Coupling Constraints. *INFORMS Journal on Optimization*, 6(1):32–45, January 2024. ISSN 2575-1492. doi: 10.1287/ijoo.2023.0005.

- Rahman Khorramfar, Dharik Mallapragada, and Saurabh Amin. Electric-gas infrastructure planning for deep decarbonization of energy systems. *Applied Energy*, 354:122176, 2024. ISSN 0306-2619. doi: <https://doi.org/10.1016/j.apenergy.2023.122176>.
- Diederik P Kingma and Max Welling. Auto-encoding variational bayes. *arXiv preprint arXiv:1312.6114*, 2013.
- Daniel Kuhn, Wolfram Wiesemann, and Angelos Georghiou. Primal and dual linear decision rules in stochastic and robust optimization. *Mathematical Programming*, 130(1):177–209, 2011.
- Henry Lam and Huajie Qian. Combating conservativeness in data-driven optimization under uncertainty: A solution path approach, 2019.
- Roberto Minguez, Raquel García-Bertrand, José M Arroyo, and Natalia Alguacil. On the solution of large-scale robust transmission network expansion planning under uncertain demand and generation capacity. *IEEE Transactions on Power Systems*, 33(2):1242–1251, 2017.
- Muhammad Ferjad Naeem, Seong Joon Oh, Youngjung Uh, Yunjey Choi, and Jaejun Yoo. Reliable fidelity and diversity metrics for generative models. In *International Conference on Machine Learning*, pages 7176–7185. PMLR, 2020.
- George Papamakarios, Eric Nalisnick, Danilo Jimenez Rezende, Shakir Mohamed, and Balaji Lakshminarayanan. Normalizing flows for probabilistic modeling and inference. *Journal of Machine Learning Research*, 22(57):1–64, 2021.
- F. Pedregosa, G. Varoquaux, A. Gramfort, V. Michel, B. Thirion, O. Grisel, M. Blondel, P. Prettenhofer, R. Weiss, V. Dubourg, J. Vanderplas, A. Passos, D. Cournapeau, M. Brucher, M. Perrot, and E. Duchesnay. Scikit-learn: Machine learning in Python. *Journal of Machine Learning Research*, 12:2825–2830, 2011.
- Said Rahal, Zukui Li, and Dimitri J. Papageorgiou. Deep lifted decision rules for two-stage adaptive optimization problems. *Computers & Chemical Engineering*, 159:107661, 2022. ISSN 0098-1354. doi: <https://doi.org/10.1016/j.compchemeng.2022.107661>.
- Albert Reuther, Jeremy Kepner, Chansup Byun, Siddharth Samsi, William Arcand, David Bestor, Bill Bergeron, Vijay Gadepally, Michael Houle, Matthew Hubbell, Michael Jones, Anna Klein, Lauren Milechin, Julia Mullen, Andrew Prout, Antonio Rosa, Charles Yee, and Peter Michaleas. Interactive supercomputing on 40,000 cores for machine learning and

- data analysis. In *2018 IEEE High Performance extreme Computing Conference (HPEC)*, pages 1–6. IEEE, 2018.
- Line A Roald, David Pozo, Anthony Papavasiliou, Daniel K Molzahn, Jalal Kazempour, and Antonio Conejo. Power systems optimization under uncertainty: A review of methods and applications. *Electric Power Systems Research*, 214:108725, 2023.
- C. Ruiz and A.J. Conejo. Robust transmission expansion planning. *European Journal of Operational Research*, 242(2):390–401, 2015. ISSN 0377-2217. doi: <https://doi.org/10.1016/j.ejor.2014.10.030>.
- Aurélie Thiele, Tara Terry, and Marina Epelman. Robust linear optimization with recourse. *Rapport technique*, pages 4–37, 2009.
- Shiwei Xie, Zhijian Hu, and Jueying Wang. Two-stage robust optimization for expansion planning of active distribution systems coupled with urban transportation networks. *Applied Energy*, 261:114412, 2020.
- Bo Zeng and Long Zhao. Solving two-stage robust optimization problems using a column-and-constraint generation method. *Operations Research Letters*, 41(5):457–461, 2013. ISSN 0167-6377. doi: <https://doi.org/10.1016/j.orl.2013.05.003>.
- Hongyu Zhang, Nicolò Mazzi, Ken McKinnon, Rodrigo Garcia Nava, and Asgeir Tomasgard. A stabilised Benders decomposition with adaptive oracles for large-scale stochastic programming with short-term and long-term uncertainty. *Computers & Operations Research*, page 106665, 2024.
- İhsan Yanikoğlu, Bram L. Gorissen, and Dick den Hertog. A survey of adjustable robust optimization. *European Journal of Operational Research*, 277(3):799–813, 2019. ISSN 0377-2217. doi: <https://doi.org/10.1016/j.ejor.2018.08.031>.

A Capacity Expansion Model

The capacity expansion model is given by

$$\min_x \sum_{i \in \mathcal{N}} c^d x_i^d + \sum_{i \in \mathcal{N}} \sum_{p \in \mathcal{P}} c^p x_i^p + \sum_{i \in \mathcal{N}} c^b x_i^b + \sum_{(i,j) \in \mathcal{E}} c^\ell x_{ij}^\ell + \lambda \max_{\xi \in \mathcal{U}} f(\xi, x) \quad (5a)$$

$$\text{s.t.} \quad \sum_{i \in \mathcal{N}} x_i^p \leq \Gamma^p \quad p \in \mathcal{P} \quad (5b)$$

$$x_i^d \leq \Gamma^d \quad i \in \mathcal{N} \quad (5c)$$

$$x_{ij}^\ell \leq \Gamma_{ij}^\ell \quad (i, j) \in \mathcal{E} \quad (5d)$$

$$x_i^d \in \mathbb{Z}^+, x_i^p, x_i^b, x_{i',j'}^\ell \in \mathbb{R}^+ \quad p \in \mathcal{P}, i \in \mathcal{N}, (i', j') \in \mathcal{E} \quad (5e)$$

Here the first-stage node-level decision variables include installed dispatchable generation capacity ($x_i^d \in \mathbb{Z}_+$), installed renewable plant capacity ($x_i^p \in \mathbb{R}_+$) for renewable technologies $p \in \mathcal{P}$, and installed battery storage capacity ($x_i^b \in \mathbb{R}_+$). Additionally, we consider transmission capacity ($x_{ij}^\ell \in \mathbb{R}_+$) as a first-stage decision variable at the link level. Both installed dispatchable generation capacities and installed renewable plant capacities obey a system-wide resource availability constraint while installed transmission capacities obey a link-level resource availability constraint. Finally, $\max_{\xi \in \mathcal{U}} f(\xi, x)$ denotes the worst-case recourse cost (i.e., economic dispatch cost given by (6)), which is incurred with unit cost λ as part of the capacity expansion objective function. We “annualize” the worst-case recourse cost by setting $\lambda = 365$. For a given investment decision x and uncertainty realization ξ , the recourse cost is given by

$$f(\xi, x) = \min_y \sum_{t \in \mathcal{T}} \sum_{i \in \mathcal{N}} c^f y_{it}^1 + c^s y_{it}^6 \quad (6a)$$

$$\text{s.t.} \quad y_{it}^1 + \sum_{j \in \mathcal{N}} y_{jit}^2 + y_{it}^3 + y_{it}^4 = \xi_{it}^d - \sum_{p \in \mathcal{P}} \xi_{it}^p x_i^p \quad i \in \mathcal{N}, t \in \mathcal{T} \quad (6b)$$

$$y_{ijt}^2 + y_{jit}^2 = 0 \quad (i, j) \in \mathcal{E}, t \in \mathcal{T} \quad (6c)$$

$$y_{ijt}^2 \leq x_{ij}^\ell \quad (i, j) \in \mathcal{E}, t \in \mathcal{T} \quad (6d)$$

$$-y_{ijt}^2 \leq x_{ij}^\ell \quad (i, j) \in \mathcal{E}, t \in \mathcal{T} \quad (6e)$$

$$y_{it}^1 \leq \nu x_i^d \quad i \in \mathcal{N}, t \in \mathcal{T} \quad (6f)$$

$$y_{it}^1 - y_{i,t-1}^1 \leq \bar{\kappa} \nu x_i^d \quad i \in \mathcal{N}, t \in \mathcal{T} \quad (6g)$$

$$y_{i,t-1}^f - y_{it}^1 \leq -\underline{\kappa} \nu x_i^d \quad i \in \mathcal{N}, t \in \mathcal{T} \quad (6h)$$

$$y_{it}^5 \leq x_i^b \quad i \in \mathcal{N}, t \in \mathcal{T} \quad (6i)$$

$$y_{it}^5 - y_{i,t-1}^5 + y_{i,t-1}^4 = 0 \quad i \in \mathcal{N}, t \in \mathcal{T} \quad (6j)$$

$$y_{it}^3 - y_{it}^6 \leq 0 \quad i \in \mathcal{N}, t \in \mathcal{T} \quad (6k)$$

$$y_{it}^1, y_{it}^5, y_{it}^6 \geq 0 \quad i \in \mathcal{N}, t \in \mathcal{T}. \quad (6l)$$

Here, the total dispatchable generation at node i in period t is denoted by y_{it}^1 . y_{ijt}^2 denotes the inflow of power from node i to node j in hour t . y_{it}^4 denotes the discharge rate of the battery located at node i in hour t while y_{it}^5 denotes its total charge. Load shedding is denoted by y_{it}^6 , which is assumed to be the positive part of y_{it}^3 . ν denotes the nameplate capacity of the dispatchable plants while $\bar{\kappa}$ and $\underline{\kappa}$ respectively denote the maximum ramp-up and ramp-down rates for dispatchable generation. The objective function (6a) minimizes the combined cost of fuel and a carbon tax for dispatchable generation (with unit cost jointly denoted by c^f) as well as load shedding (with unit cost c^s). First-stage decisions x_i^d , x_i^p , x_i^b , and x_{ij}^l parameterize the constraints of (6). Constraints (6b) impose flow conservation at each node. Specifically, the constraint balances dispatchable generation, power inflows, nodal load shedding, and battery discharging with net load (i.e., demand minus total generation from renewables). Importantly, y_{ijt}^2 is negative if node j receives power from node i , which is captured by the equality constraint (6c). Constraints (6d) and (6e) impose line limits on power flows. Constraints (6f) impose limits on total dispatchable generation while constraints (6g) and (6h) limit ramping up and down of dispatchable generation. Constraints (6i) limits the total state-of-charge of batteries. Constraints (6j) links battery discharging or charging (taken to be the negative of discharging) rates to battery state-of-charge. Constraints (6k) ensure that only the positive part of load shedding incurs a cost.

B Experimental Setup Details

B.1 Data Processing

To process the data, we remove components corresponding to solar capacity factors for nighttime hours and offshore wind capacity factors for landlocked nodes, both of which correspond to capacity factors of zero in all observations, which gives $\xi \in \mathbb{R}^{427}$. In implementing CCG, we also remove redundant (i.e., perfectly multicollinear) components so that the dataset of ξ observations has full column rank when defining the uncertainty set. We then re-introduce the redundant components as affine transformations of the retained components in the adversarial subproblem using equality constraints. Consequently, the effective dimensionality of \mathcal{U} is 349 while the dimensionality of ξ is 427. For AGRO, we only remove components that are constant (i.e., zero) and train the VAE on the original 427-dimensional dataset.

B.2 Computational Details

VAE training. To obtain AGRO results, we train a 4-layer VAE and evaluate a range of latent space dimensionalities, $L \in \{2, 4, 8, 16\}$. Each hidden layer has 64 hidden units and uses ELU activations. All models were trained with the Adam optimizer on a batch size of 2048 for 10000 epochs.

Optimization details. For the CCG subproblem, we introduce trivial valid inequalities in the subproblem to reduce computational runtimes. To solve the adversarial subproblem for AGRO, we assume a step size of $\eta = 0.01$ and terminate the subproblem when subsequent iterations of gradient ascent yield less than 0.001% change in cost or when 100 iterations have been performed. We perform at least $I = 3$ initializations of the subproblem in each iteration of AGRO but perform additional initializations (up to a maximum of 10 total) if the solution to the adversarial subproblem does not increase costs over the current estimate of worst-case recourse costs (i.e., if $f(\xi^i, x^*) < \gamma$).

Computational resources. Optimization results for the AGRO subproblem are obtained using the Cvxpylayers package [Agrawal et al., 2019] while results for the AGRO and CCG main problems as well as the CCG subproblem are obtained using Gurobi 11.0 [Gurobi Optimization, LLC, 2023] with a mixed-integer optimality gap of 0.01%. All optimization and model training is performed on the MIT Supercloud system [Reuther et al., 2018] using an Intel Xeon Gold 6248 machine with 40 CPUs and two 32GB NVIDIA Volta V100 GPUs.

B.3 VAE Performance Metrics

We quantify sampling performance of the VAE using standard metrics for fidelity (precision and density) and diversity (recall and coverage). These metrics are defined by Naeem et al. [2020] as follows:

$$\begin{aligned} \text{precision} &= \frac{1}{M} \sum_{j=1}^M \mathbb{1}_{\hat{\xi}_j \in \text{manifold}(\xi_1, \dots, \xi_N)} \\ \text{density} &= \frac{1}{kM} \sum_{j=1}^M \sum_{i=1}^N \mathbb{1}_{\hat{\xi}_j \in \mathcal{B}(\xi_i, \text{NND}_k(\xi_i))} \\ \text{recall} &= \frac{1}{N} \sum_{i=1}^N \mathbb{1}_{\xi_i \in \text{manifold}(\hat{\xi}_1, \dots, \hat{\xi}_M)} \\ \text{coverage} &= \frac{1}{N} \sum_{i=1}^N \mathbb{1}_{\exists j \text{ s.t. } \hat{\xi}_j \in \mathcal{B}(\xi_i, \text{NND}_k(\xi_i))} \end{aligned}$$

where ξ and $\hat{\xi}$ respectively denote real (N total) and generated samples (M total), $\mathbb{1}$ denotes the indicator function, $\text{NND}_k(\xi_i)$ denotes the distance from ξ_i to its k -th nearest neighbor (excluding itself) in the dataset $\{\xi_1, \dots, \xi_N\}$, and manifolds are defined as

$$\text{manifold}(\xi_1, \dots, \xi_N) = \bigcup_{i=1}^N \mathcal{B}(\xi_i, \text{NND}_k(\xi_i)).$$

Precision and density quantify the portion of generated samples that are “covered” by the real samples while recall and coverage quantify the portion of real samples that are “covered” by the generated samples. All results in Table 3 are obtained using $k = 5$ and with $M = N = 1260$.